International Journal of Applied Science and Engineering

# Initial turbidity, pH, dosage of alum and paddles type optimization of efficiency removal by using response surface methods (RSM)

**Zainb Abd alelah Abd Alateef, Fatma Abd Alemam Jyad, Maha Atta Faroon, Ahmed Naseh Ahmed Hamdan** *

*Department of Civil Engineering, College of Engineering, University of Basrah, Basrah 61001, Iraq*

## ABSTRACT

Response Surface Methods (RSM) and desirability functions are good examples of data-based multivariate methods that can be used to study coagulation treatment optimization. This study examined and optimized the efficacy of turbidity reduction, under the operating conditions of initial turbidity $T_{in}$ (50–200 NTU), pH (5–9), and alum dose (50–250 mg/L) for two types of fan (two paddles and four paddles) using Face-Centered Central Composite Design F-CCCD of RSM. The experimental results of F-CCCD were fitted to the second-order quadratic model for the two types of fans in order to formulate the impacts of each element and their interactions on the response of interest in a mathematical connection. The results showed that at optimal operating conditions for a fan with two paddles of $T_{in}$, pH and alum dose of 87.76 NTU, 8.86 and 170.43 mg/L, respectively, the predicted values of turbidity removal efficiency (E%) was 85.92% and for four paddles fan type when $T_{in}$, pH and alum dose of 156.58 NTU, 8.93, and 138.7 mg/L, respectively, the predicted values of turbidity removal efficiency (E%) was 93.71, with the desirability of 1.000. This study showed how well F-CCCD works with a desirability function to find the best conditions for the process ($T_{in}$, pH, and alum dosage) of coagulation for the turbidity removal efficiency E%. A four-paddle fan type provided the best removal efficiency. Instead of jar testing, drinking water treatment companies might utilize the findings of this study as a starting point for their work.

***Keywords:*** Flocculation, Efficiency removal, Coagulation, Central composite design, Response surface method, Optimization network (ANN).

**OPEN ACCESS**

**Received:** December 16, 2022
**Revised:** June 28, 2023
**Accepted:** October 7, 2023

**Corresponding Author:**
Ahmed Naseh Ahmed Hamdan
ahmed.hamdan@uobasrah.edu.iq



**Publisher:**
Chaoyang University of Technology
**ISSN:** 1727-2394 (Print)
**ISSN:** 1727-7841 (Online)

## 1. INTRODUCTION

Turbidity is a way to measure how many particles are in the water, and too many particles can make the water unsafe for drinking, swimming, and aquatic life. Turbidity removal is the process of lowering the amount of these particles in water to a level that is acceptable. By getting particles to stick together, chemical processes like coagulation and flocculation can make physical processes work better. The connections between raw water and process factors are complicated and not straight lines. Changes in the chemical make-up of raw water and the physical properties of the coagulation-flocculation event can affect how water is treated. Silicate, pH, temperature, the amount of coagulant used, natural process conditions, and the hydraulic dynamics of the treatment water flow are all significant factors in the water treatment process (Shi et al., 2007; Xiao et al., 2009; Miron et al., 2010).

The effectiveness of the selection and usage of coagulants for the treatment of water has been evaluated using the jar test technique. Because it does not examine the complete practical space for the interactions of all factors that impact coagulation, this experimental procedure is constrained in identifying the ideal circumstances for therapy

(Zainal-Abideen et al., 2012). Due to its accessibility, and safety, handling aluminum sulphate is the preferred coagulant in the jar test experiment. Natural coagulation treatment parameters include aluminum sulphate (alum) as a key factor. However, starting turbidity and pH both have an impact on how effective coagulation solutions are. The fan type was changed from a two-paddle fan to a four-paddle fan, and all experiments were repeated with this type to determine its effect on the amount of turbidity removal. One of the most effective statistical methods to use is the multivariate statistical methodology after executing the jar test experiment to evaluate a coagulant's acceptability and effectiveness for use in water treatment.

As water treatment procedures are optimized, both treatment effectiveness and cost are raised and decreased (Rachidi et al., 2021; Rohani et al., 2021). Recently, a number of techniques have been used for modeling and optimization of the coagulation-flocculation process, such as generalized regression neural network, and RSM. Process of coagulation and flocculation RSM is a statistical technique for optimizing and enhancing the performance of a system or process. It entails designing experiments to collect data and constructing a mathematical model to depict the relationship between the input variables (factors) and the outcome variable (the response). RSM's objective is to determine the optimal input variable values that will produce the best output or response. By employing mathematical models, RSM can aid in identifying the essential output-affecting elements and their interactions, as well as the optimal process conditions, hence minimizing experimental time and expense (Karchiyappan and Karri, 2021; Perec, 2021). RSM Technique is a fairly new way to improve a process. It includes planning an experiment, analyzing it, and using partial regression to model the parameters of the experiment. The coagulation-flocculation method was used by Usefi and Asadi-Ghalhari (2019) to eliminate turbidity using rice starch, and the system was optimised using the central composite design (CCD) approach. The findings showed that at the optimal point, 98.4% of the turbidity was removed. Furthermore, among the four independent variables (pH, settling time, rice starch dosage, and slow mixing), they discovered that pH had the most significant impact on turbidity removal (Usefi and Asadi-Ghalhari, 2019). To find the optimal operating conditions with the jar test, Zainal-Abideen et al. (2012) compared the conventional one-factor-at-a-time method with RSM. Final turbidity, pH, and residual aluminum were examined as a function of initial pH, alum dosage, and polymer dose. The RSM employed a randomised, centred, composite design with 18 independent trials and 4 central replicates. The research demonstrated that the RSM method produced coagulated water of comparable and acceptable quality despite using lesser alum and polymer dosages than the conventional method (Zainal-Abideen et al., 2012). The effectiveness of alum and poly-aluminum chloride in the coagulation of waste leachate was compared by Ghafari et al. (2009) using RSM. Coagulant dose and pH were examined as potential causes, and reductions in chemical oxygen demand (COD), turbidity, colour, and total suspended solids were evaluated as potential effects. Alum was more effective at removing COD, but PACl was better at removing turbidity, colour, and total suspended solids (Ghafari et al., 2009).

Together, professionals in water treatment engineering, chemistry, and statistics can build effective and efficient coagulation techniques for turbidity reduction in water treatment. The primary objective of this study is to analyze the previously identified process variables that influence the water coagulation process. RSM was used to evaluate the effects of fan type and three factors (initial turbidity $T_{in}$, pH, and alum dose (Dosage) on turbid water turbidity reduction.

## 2. MATERIALS AND METHODS

Distilled water was used in this study to exclude any potential influence from water-based factors on turbidity reduction. Kaolin powder creates the needed turbidity in a synthetic fashion by adding the kaolin powder to distilled water until the required turbidity is reached. Sulfuric acid and sodium hydroxide were used to balance the pH. Aluminum sulfate $Al_2(SO_4)_3{\cdot}18H_2O$, the most common type of coagulant found in many water treatment plants in Iraq, was used in the current study. Experiments on jars were conducted within the ranges of pH 5 to 9, initial turbidity ($T_{in}$) 50 to 200 NTU, and alum dosage 50 to 250 mg/L. The samples were placed in a 1000 mL beaker and swirled for one min at 100 rpm (rapid mixing). For 20 min, the mixing speed was dropped to 40 rpm for flocculation (slow mixing). Each floc that formed was given 30 min to settle. To measure the turbidity, samples of the water were taken from 20 mm below the surface. Nephelometric Turbidity Units were used to measure the turbidity of the supernatant with a HACH 2100A turbid meter (NTU). Final turbidity was used to measure how well the system worked, and the % removal efficiency with aluminum sulfate was calculated using Equation 1. Two types of fans were used to see how they affected coagulation and flocculation processes and how well got rid of turbidity. In Fig. 1, type (1) has two paddles, and type (2) has four paddles. Kang and Cleasby (2015) said that low temperatures can slow down the rate of coagulation and flocculation, so the temperature of the room was used for the tests. Table 1 gives a summary of the things that happened during the jar tests.

$$(Removal\ Efficiency)E(\%) = \left[\left(T_{in} - T_{fin}\right)/T_{in}\right] * 100 \quad (1)$$

Where; $T_{in}$ is initial turbidity, $T_{fin}$ is final turbidity, and $E$ is removal efficiency.

Minimum, maximum, and average values were taken for the three variables ($T_{in}$, pH, and alum dosage) and the values were entered into the RSM (Table 2), which in turn prepared a table of the necessary experiments to obtain the output,

International Journal of Applied Science and Engineering



removal efficiency E% (Table 3). Experiments were conducted using the jar test with the mixing time and speed fixed for all experiments and for a fan of two paddles. Then all the required experiments were repeated under the same conditions using a fan of four paddles.

In an experiment with only one variable, the coagulation conditions are changed while all other variables stay the same (Zainal-Abideen et al., 2012). RSM was used to find the best combinations of the factors that affect how well the coagulation process works. The experiment was set up and the data were analyzed with the help of the statistical software Design Expert 13.0. Face Centered Central Composite Design F-CCCD was used for each fan type to find the best way for the initial turbidity ($T_{in}$), pH, and alum dosage to work together. Table 2 shows the ranges and level codes for each variable (factor). The answer from the design was removal efficiency (E %), which stood for. There were 40 test runs, with 20 for each type of fan.

The F-CCCD in this study has 8 factorial points, 6 axial (star) points, and 6 center points, with 20 experimental runs for each fan type. Additionally, the F-CCCD can be used to fit quadratic response surfaces and optimize response processes (Salehi et al., 2010; Alam et al., 2016). This experiment's reaction surface F-CCCD data were fitted to the quadratic model for each fan type in order to determine the relationship between the variable components (*A, B*, and *C*) and the response removal efficiency *E*% using the generalized version of second-order-multiple-regression-Equation 2.

$$E(\%) = \alpha_0 + \alpha_1 A + \alpha_2 B + \alpha_3 C + \alpha_{12} AB + \alpha_{13} AC + \alpha_{23} BC + \alpha_{11} A^2 + \alpha_{22} B^2 + \alpha_{33} C^2 \quad (2)$$

where *E* (%) represents the response model (efficiency removal %); $\alpha_0$, $\alpha_1$, $\alpha_2$ are the coefficients associated with the intercept, the linear term, the quadratic term, and the interaction effect term, respectively; *A, B*, and *C* are the independent variables in coded form (Factors). Analysis of variance (ANOVA), a type of statistical analysis, was used to look at how the different factors and their responses interact with each other. At the 95% confidence level, the determination coefficient ($R^2$) and the lack of fit value (p-value) were used to see how well the second-order

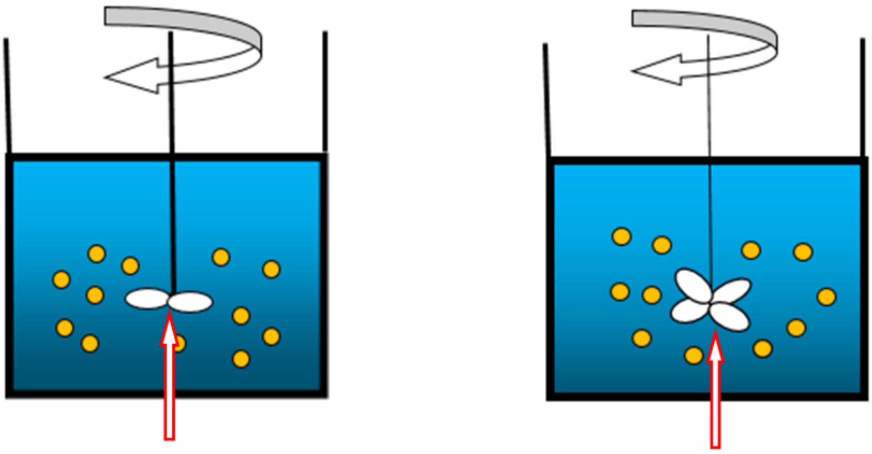


**Fig. 1.** The two types of fans used in the experiments

**Table 1.** Jar test experiment characteristics

| Characteristics | Description |
|---|---|
| Initial turbidity ($T_{in}$) | 50–200 NTU |
| pH | 5–9 |
| Aluminum sulfate dose | 50–250 mg/L |
| Type of fan | Two paddles and four paddles |
| Rapid mixture | 1 min at 100 rpm |
| Slow mixture | 20 min at 40 rpm |
| Settling | 30 min |

**Table 2.** Experimental factors and their coded levels for each fan type

| Factors | Unit | Symbols | Type | Low level (-1) | Center level (0) | High level (+1) |
|---|---|---|---|---|---|---|
| $T_{in}$ | NTU | A | Numeric | 50 | 125 | 200 |
| pH | | B | Numeric | 5 | 7 | 9 |
| Dosage | mg/L | C | Numeric | 50 | 150 | 250 |

polynomial model fit the two types of fans. The fitted models were used to make contour plots, which were used to predict that the variable parameters ($T_{in}$, pH, and Alum dosage) could be optimized to get the best removal efficiency *E* (%) within the range of values that were given.

## 2. RESULTS AND DISCUSSION

The F-CCCD experimental data for each fan type, including the number of runs, the axial points, and the corresponding factor variables ($T_{in}$, pH, and Alum dosage), as well as the response (removal efficiency E%), are shown in Table 3. To choose the right model from the linear, two-factor interaction (2FI), quadratic, and cubic response models that describe how the variables affect the process responses, the quality of each model was tested for each fan type using statistical indices like coefficient of determination $R^2$, adjusted $R^2$ which equal to $\left[1-(1-R^2)\frac{(n-1)}{(n-m-1)}\right]$ (where; *n*: total number of samples, *m*: the number of variables that are independent), and predicted $R^2$ as shown in Tables 4 and 5.

As shown in Table 6, the $R^2$ values for the two types of fans for removal efficiency E (%) were 0.9538 and 0.9452, which are very close to 1. There was a good match between the predicted $R^2$ values and the adjusted $R^2$ values for removal efficiency E (%) in the response quadratic model's equations, with a difference of less than 0.2. In the same way, the fact that both 16.4360 and 13.2992 for E (%) are greater than 4 shows that each model can move around in the design space. So, these results show that the experimental data are reliable and that the models can be used to estimate the E (%) (Haji Alhaji et al., 2017). A diagnostic test to see if the proposed model is good enough is done using ANOVA, as shown in Table 6. At a 95% confidence level, the model that was made is significant. Reproducibility is met by the fact that the CV values for the removal efficiency (E %) model are less than 10%.

**Table 3.** Factors and their response according to F-CCCD for the two fan types

| Run | Space type | $T_{in}$ | pH | Dosage | E % for a fan of two paddles | E % for a fan of four paddles |
|---|---|---|---|---|---|---|
| 1 | Center | 125 | 7 | 150 | 62.9 | 90.9 |
| 2 | Center | 125 | 7 | 150 | 55.2 | 89.3 |
| 3 | Center | 125 | 7 | 150 | 51.6 | 84.5 |
| 4 | Center | 125 | 7 | 150 | 69.3 | 79.9 |
| 5 | Center | 125 | 7 | 150 | 59.1 | 77.0 |
| 6 | Center | 125 | 7 | 150 | 60.7 | 79.8 |
| 7 | Axial | 125 | 7 | 250 | 54.1 | 77.3 |
| 8 | Axial | 50 | 7 | 150 | 65.8 | 71.6 |
| 9 | Axial | 200 | 7 | 150 | 53.9 | 74.8 |
| 10 | Axial | 125 | 7 | 50 | 51.2 | 79.6 |
| 11 | Axial | 125 | 9 | 150 | 85.6 | 92.1 |
| 12 | Axial | 125 | 5 | 150 | 48.2 | 77.0 |
| 13 | Factorial | 200 | 9 | 50 | 72.7 | 80.2 |
| 14 | Factorial | 50 | 9 | 250 | 80.2 | 49.3 |
| 15 | Factorial | 50 | 5 | 250 | 33.6 | 37.8 |
| 16 | Factorial | 50 | 5 | 50 | 35.6 | 45.0 |
| 17 | Factorial | 200 | 9 | 250 | 71.8 | 68.9 |
| 18 | Factorial | 200 | 5 | 250 | 29.7 | 34.6 |
| 19 | Factorial | 50 | 9 | 50 | 78.6 | 56.9 |
| 20 | Factorial | 200 | 5 | 50 | 30.3 | 38.0 |

**Table 4.** Statistics of model selection for E (%) for fans of two paddles

| Source | Sequential p-value | Lack of fit p-value | Adjusted $R^2$ | Predicted $R^2$ | Remark |
|---|---|---|---|---|---|
| Linear | < 0.0001 | 0.5573 | 0.8647 | 0.8335 | |
| 2FI | 0.9907 | 0.3996 | 0.8348 | 0.6192 | |
| Quadratic | 0.0251 | 0.914 | 0.9122 | 0.8819 | Suggested |
| Cubic | 0.8905 | 0.5651 | 0.8756 | -2.4477 | Aliased |

**Table 5.** Statistics of model selection for E (%) for fans of four paddles

| Source | Sequential p-value | Lack of fit p-value | Adjusted $R^2$ | Predicted $R^2$ | Remark |
|---|---|---|---|---|---|
| Linear | 0.2199 | 0.0046 | 0.0917 | -0.4380 | |
| 2FI | 0.8013 | 0.0028 | -0.0380 | -4.5478 | |
| Quadratic | < 0.0001 | 0.3949 | 0.8959 | 0.788 | Suggested |
| Cubic | 0.8445 | 0.0919 | 0.8583 | -24.5523 | Aliased |

**Table 6.** Fit statistics for removal efficiency E (%) for the two types of fans

| Four paddles | | | | Two paddles | | | |
|---|---|---|---|---|---|---|---|
| Std. Dev. | 6.01 | $R^2$ | 0.9452 | Std. Dev. | 4.9 | $R^2$ | 0.9538 |
| Mean | 69.23 | Adjusted $R^2$ | 0.8959 | Mean | 57.51 | Adjusted $R^2$ | 0.9122 |
| C.V. % | 8.69 | Predicted $R^2$ | 0.7880 | C.V. % | 8.52 | Predicted $R^2$ | 0.8819 |

The proposed model is put to the test using ANOVA, as shown in Table 6. The model that was made is significant with a 95% level of confidence. Reproducibility is met by the removal efficiency E (%) model because the CV values are less than 10%. Thus, it was determined that the quadratic model provided the greatest match to the experimental F-CCCD data, with a high connection between the variable components and their respective answers. Equations 3 and 4 offer the coded quadratic polynomial equations and actual values.

For fans of two paddles:

$$E(\%) = 60.63 - 3.54A + 21.15B + 0.10C - 0.64\,AB - 0.14AC + 0.41BC - 2.04A^2 + 5.01B^2 - 9.24C^2 \quad (3)$$

For fans of four paddles:

$$E(\%) = 86.15 + 3.59A + 11.5B - 3.18C + 6.64AB + 0.01255AC - 1.04BC - 16.81A^2 - 5.46B^2 - 11.56C^2 \quad (4)$$

where, E (%) is removal efficiency; *A, B*, and *C* are initial turbidity $T_{in}$, pH, and Alum dose (Dosage), in coded units, respectively.

In order to evaluate the models' efficacy, the F-value and P-value were calculated. The model appears to be significant, as indicated by the model F-values of 22.93 and 19.18 in Tables 7 and 8. P-values for model terms under 5% are deemed significant and support the existence of factor response interactions. The operational parameters, experimental outcomes, and anticipated data are displayed in Table 9. The outcomes in Table 9 demonstrated that the experimental data fit the model exactly.

**Table 7.** ANOVA for Quadratic model for two paddles

| Source | Sum of squares | df | Mean square | F-value | p-value | |
|---|---|---|---|---|---|---|
| Model | 4950.12 | 9 | 550.01 | 22.93 | < 0.0001 | Significant |
| A-$T_{in}$ | 125.32 | 1 | 125.32 | 5.22 | 0.0454 | |
| B-pH | 4473.22 | 1 | 4473.22 | 186.46 | < 0.0001 | |
| C-Dosage | 0.1 | 1 | 0.1 | 0.0042 | 0.9498 | |
| AB | 3.25 | 1 | 3.25 | 0.1355 | 0.7204 | |
| AC | 0.1512 | 1 | 0.1512 | 0.0063 | 0.9383 | |
| BC | 1.36 | 1 | 1.36 | 0.0567 | 0.8165 | |
| $A^2$ | 11.4 | 1 | 11.4 | 0.4753 | 0.5062 | |
| $B^2$ | 69.13 | 1 | 69.13 | 2.88 | 0.1205 | |
| $C^2$ | 234.6 | 1 | 234.6 | 9.78 | 0.0107 | |
| Residual | 239.91 | 10 | 23.99 | | | |
| Lack of Fit | 50.35 | 5 | 10.07 | 0.2656 | 0.914 | Not significant |
| Pure Error | 189.56 | 5 | 37.91 | | | |
| Cor total | 5190.03 | 19 | | | | |

**Table 8.** ANOVA for Quadratic model for four paddles

| Source | Sum of squares | df | Mean square | F-value | p-value | |
|---|---|---|---|---|---|---|
| Model | 6241.72 | 9 | 693.52 | 19.18 | < 0.0001 | Significant |
| A-$T_{in}$ | 128.88 | 1 | 128.88 | 3.56 | 0.0884 | |
| B-pH | 1322.50 | 1 | 1322.50 | 36.57 | 0.0001 | |
| C-dosage | 101.12 | 1 | 101.12 | 2.80 | 0.1254 | |
| AB | 352.45 | 1 | 352.45 | 9.75 | 0.0108 | |
| AC | 0.0012 | 1 | 0.0012 | 0.0000 | 0.9954 | |
| BC | 8.61 | 1 | 8.61 | 0.2381 | 0.6361 | |
| $A^2$ | 777.42 | 1 | 777.42 | 21.50 | 0.0009 | |
| $B^2$ | 82.09 | 1 | 82.09 | 2.27 | 0.1628 | |
| $C^2$ | 367.72 | 1 | 367.72 | 10.17 | 0.0097 | |
| Residual | 361.67 | 10 | 36.17 | | | |
| Lack of fit | 203.40 | 5 | 40.68 | 1.29 | 0.3949 | Not significant |
| Pure error | 158.27 | 5 | 31.65 | | | |
| Cor total | 6603.40 | 19 | | | | |

**Table 9.** Actual and predicted responses data F-CCCD

| Run | $T_{in}$ NTU | pH | Dosage mg/L | Actual E (%) for a fan of two paddles | Predicted E (%) for a fan of two paddles | Actual E (%) for a fan of four paddles | Predicted E (%) for a fan of four paddles |
|---|---|---|---|---|---|---|---|
| 1 | 125 | 7 | 150 | 62.90 | 60.63 | 90.90 | 86.15 |
| 2 | 125 | 7 | 150 | 55.20 | 60.63 | 89.30 | 86.15 |
| 3 | 125 | 7 | 150 | 51.60 | 60.63 | 84.50 | 86.15 |
| 4 | 125 | 7 | 150 | 69.30 | 60.63 | 79.90 | 86.15 |
| 5 | 125 | 7 | 150 | 59.10 | 60.63 | 77.00 | 86.15 |
| 6 | 125 | 7 | 150 | 60.70 | 60.63 | 79.80 | 86.15 |
| 7 | 125 | 7 | 250 | 54.10 | 51.50 | 77.30 | 71.40 |
| 8 | 50 | 7 | 150 | 65.80 | 62.14 | 71.60 | 65.74 |
| 9 | 200 | 7 | 150 | 53.90 | 55.06 | 74.80 | 72.92 |
| 10 | 125 | 7 | 50 | 51.20 | 51.30 | 79.60 | 77.76 |
| 11 | 125 | 9 | 150 | 85.60 | 86.80 | 92.10 | 92.18 |
| 12 | 125 | 5 | 150 | 48.20 | 44.50 | 77.00 | 69.18 |
| 13 | 200 | 9 | 50 | 72.70 | 70.97 | 80.20 | 78.24 |
| 14 | 50 | 9 | 250 | 80.20 | 80.35 | 49.30 | 49.35 |
| 15 | 50 | 5 | 250 | 33.60 | 35.95 | 37.80 | 41.70 |
| 16 | 50 | 5 | 50 | 35.60 | 36.60 | 45.00 | 46.01 |
| 17 | 200 | 9 | 250 | 71.80 | 71.72 | 68.90 | 69.83 |
| 18 | 200 | 5 | 250 | 29.70 | 29.87 | 34.60 | 35.63 |
| 19 | 50 | 9 | 50 | 78.60 | 79.05 | 56.90 | 57.81 |
| 20 | 200 | 5 | 50 | 30.30 | 30.77 | 38.00 | 39.89 |

Diagnostic plots were used to make sure that the quadratic models were close enough to the real systems to be useful. The normal probability plots in Fig. 2 evaluate how normal the model's residuals are, while the expected normal value vs. observed value plot in Fig. 3 shows the relationships between actual values and those anticipated by the removal efficiency (E%). If the data clusters around the straight line when normal-percentage-probability-values are plotted against the externally studentized residuals, the distribution is well-defined and there is no variance deviation (Pal et al., 2014; Thirugnanasambandham et al., 2015). Similarly, the dispersion of the data points for each response in the plots of expected versus observed values Fig. 3 and their proximity to one another show that the experimental data and projected values for removal efficiency (E%) are in reasonable agreement.

Figs. 4 and 5 show a 3D surface plot of the separate quadratic models of the two types of fans and how they interact. The two figures showed the close relationship between the three factors (initial turbidity, pH, and alum dose) as mentioned earlier by Kalavathy and Giridhar (2016). The two plots illustrate that when pH decreases, so does the efficiency of eliminating turbidity; adding more alum does not improve the removal work, but rather makes it less effective. If the initial turbidity increases, the removal efficiency (E %) decreases.

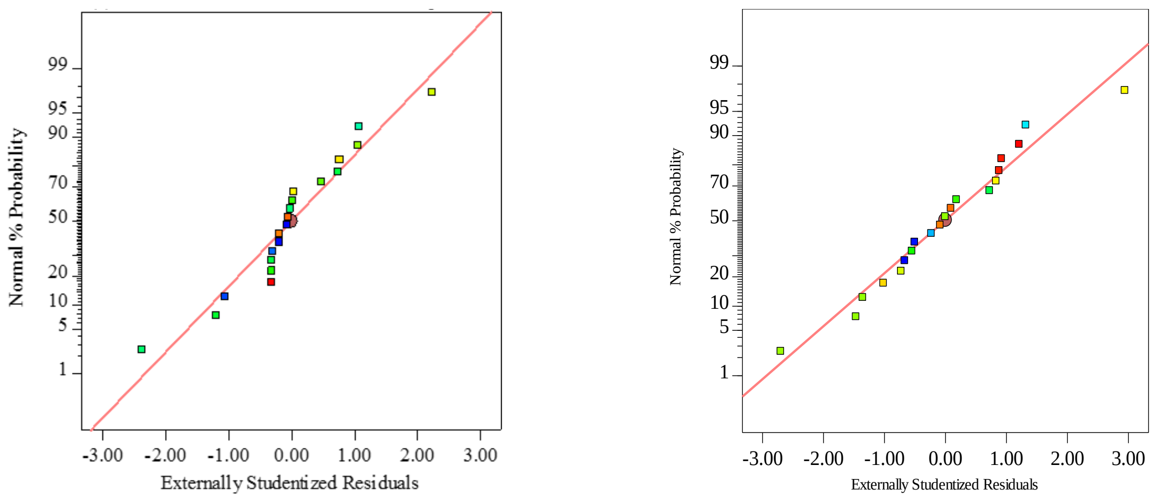


(a) (b)

**Fig. 2.** Normal- probability- plot of the residuals for (a) removal efficiency E (%) for a fan of two paddles. (b) removal efficiency E (%) for a fan of four paddles

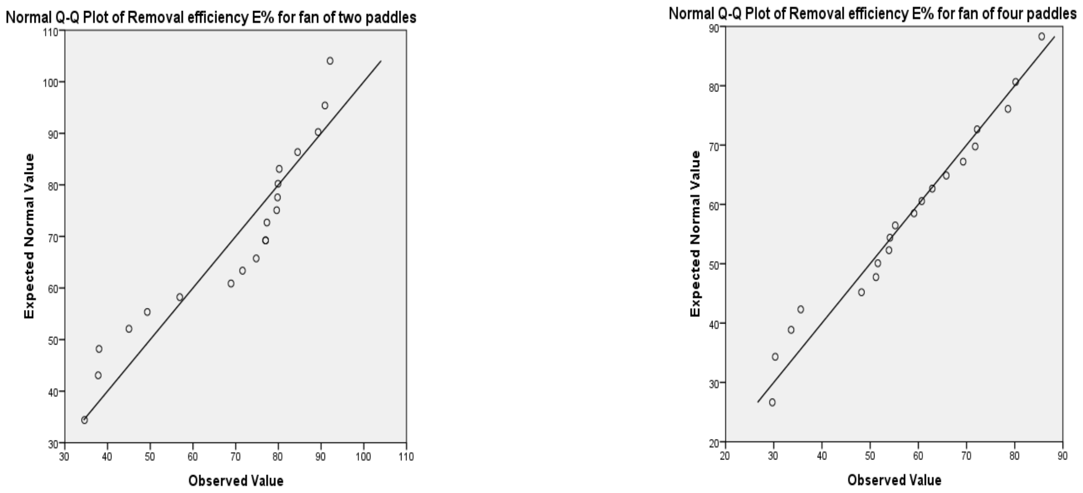


(a) (b)

**Fig. 3.** Expected normal value vs. observed value plots for (a) removal efficiency E (%) for a fan of two paddles, and (b) removal efficiency E (%) for a fan of four paddles

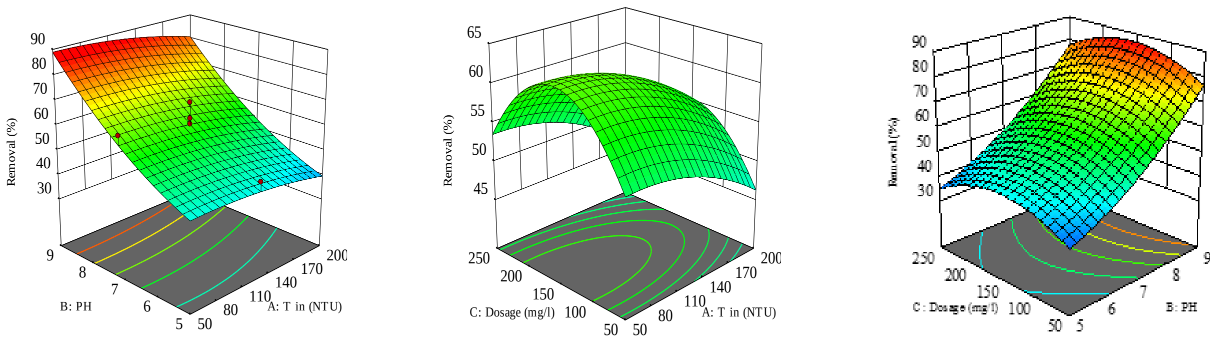


(a) (b) (c)

**Fig. 4.** Responsive three-dimensional surface and contour graphs for the effects of (a) $T_{in}$ and pH. (b) $T_{in}$ and dosage, and (c) pH and dosage on the removal efficiency E (%) for a fan of two paddles

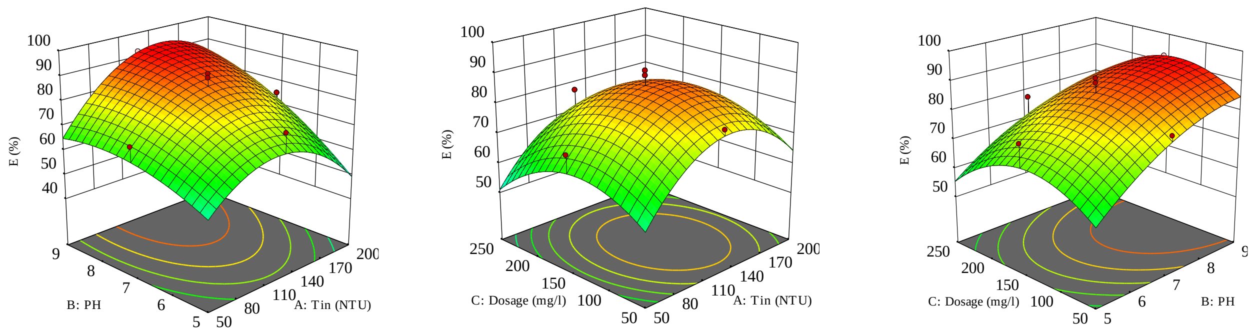


(a) (b) (c)

**Fig. 5.** Responsive three-dimensional surface and contour graphs for the effects of (a) $T_{in}$ and pH. (b) $T_{in}$ and dosage, and (c) pH and dosage on the removal efficiency E (%) for a fan of four paddles

Figs. 4 and 5, also showed how starting turbidity has an impact on removal efficiency. It was noted that the system's removal effectiveness improved as initial turbidity increased approximately from 50 to 140 NTU, but that it declined as initial turbidity increased from 140 to 200 NTU. The reduced particle size, which makes flocs smaller and less likely to settle, maybe the cause of the decreased turbidity removal at low beginning turbidity (50 NTU) (Camacho et al., 2017). Moringa oleifera seeds have been shown by Senthil et al. (2016) to filter out sediment from groundwater. The findings proved beyond any reasonable doubt that a rise in initial turbidity from 50 to 135 NTU led to a corresponding rise in removal efficiency from 54.67 to 74.28%. This suggests that increased interaction between coagulants and colloidal particles occurs at higher turbidity concentrations (Senthil et al., 2016). Instead of using the standard jar test, Kalavathy and Giridhar (2016) adopted manual agitation under extremely low settling time circumstances to determine the efficacy of two different alum doses (10 and 20 mg/L) in 250 mL of synthetic high turbid water at room temperature (pH = 6–7.4). Studies showed that the coagulation process could successfully remove turbidity with low amounts of alum (Kalavathy and Giridhar, 2016). Trinh and Kang (2010) found that employing F-CCCD was superior to conventional methods for improving coagulation. Removal efficiencies of turbidity were expressed in terms of two factors: alum dose and coagulation pH. In terms of reducing turbidity, treatment efficacy was found to be highly influenced by both pH and alum dosage. Removal of 92.5 percent of turbidity with 44 mg/L alum at pH 7.6 was determined to be optimum (Trinh and Kang, 2010). In emergency situations, excessively turbid water was removed by Nayeri and Mousavi (2020) using the coagulation-flocculation technique. The $T_{in}$ (10–350) NTU, pH (5–9), coagulant dosage (50–250 mg/L), rapid mixing (120–280) rpm, slow mixing (30–50) rpm, and sedimentation time (10–50) min were among the numerical factors whose effects were optimized using the Central-Composite-Design CCD within the framework of RSM. The information demonstrated that the ideal circumstances for turbidity removal (E%) of 99.14% were a pH of 9, an alum dosage of 50 mg/L, a $T_{in}$ of 350 NTU, quick mixing at 280 rpm, slow mixing at 50 rpm, and a sedimentation time 50 min (Nayeri and Mousavi, 2020).

Numerical optimization lets you choose a good value for every input component and response in the form of a target, range, maximum, or minimum value. $T_{in}$, pH, and dosage were set between 50 and 200 (NTU), 5 and 9 (pH), and 50 and 250 mg/L, respectively, for maximum turbidity removal efficiency E%. With the mentioned predetermined objective conditions, the F-CCCD experiment results generated the ideal processing conditions of $T_{in}$, pH, and dosage as 84.84 NTU, 8.83, and 136.557 mg/L for maximum removal efficiency E% for fan of two paddles and 144.382 NTU, 8.35, and 146.15 mg/L for the four paddles fan type. The projected removal efficiencies under the chosen conditions were 85.63% for the fan of two paddles and 92.50% for the fan of four paddles, with a desirability value of 1.000. The highest removal efficiency was attained when a four-paddle fan was used.

To make sure that the results of the optimization were correct, a confirmation experiment was done with the optimum conditions found by the F-CCCD model and three copies of each fan type. The removal efficiency E (%) at optimal process conditions was 83.95 % ± 1.56% for two paddles and 91.52 % ± 1.53% for four paddles. The results showed that the predicted model values of 85.63% and 92.50% for removal efficiency for fans with two paddles and four paddles, respectively, were very close to the real values. The results showed that F-CCCD with a desirability function worked well to find the best process conditions ($T_{in}$, pH, and dosage) for coagulation to get the best removal efficiency.

## 4. CONCLUSION

RSM is a helpful tool for performing, evaluating, and deriving conclusions from experiment results. This study looked at the operating process conditions, such as $T_{in}$, pH, and alum dosage, in water treatment using F-CCCD of RSM. Using F-CCCD experiment results, the combined effects of process variable factors on the response of interest (removal efficiency) were studied. According to the coefficients of determination and lack-of-fit tests, the results fit well with the second-order polynomial regression model. Similarly, the statistical ANOVA demonstrated that the three variable components investigated have individual and combined effects on the response of interest. Using the Derringer's desire function, the optimal process settings to optimize the removal efficiencies were determined. The optimal operating conditions with a desirability value of 1.000 were determined to be 84.84 of $T_{in}$ NTU, 8.83 of pH, and 136.56 mg/L of alum dosage, which achieved the predicted of removal efficiency (85.63%), for a fan of two paddles and 144.38 of $T_{in}$ NTU, 8.35 of pH, and 146.15 mg/L of alum dosage, which achieved the predicted removal efficiency of 92.50%. A four-paddle fan type provided the best removal efficiency.

## ACKNOWLEDGMENT

This research would like to thank the support of the University of Basrah, College of Engineering.

## REFERENCES

Alam, M.M., Alam, M.Z., Jami, M.S., Amosa, M.K., Iwata, M. 2016. Study of the effects of process parameters on electroforced sedimentation in solid–liquid separation using response surface methodology. Waste Biomass Valorization, 7, 583–591.

Camacho, F.P., Sousa, V.S., Bergamasco, R., Teixeira, M.R. 2017. The use of Moringa oleifera as a natural coagulant in surface water treatment. Chemical Engineering Journal, 313, 226–237.

Ghafari, S., Aziz, H.A., Isa, M.H., Zinatizadeh, A.A. 2009. Application of response surface methodology (RSM) to optimize coagulation–flocculation treatment of leachate using poly-aluminum chloride (PAC) and alum. Journal of Hazardous Materials, 163, 650–656.

Gasemloo, S., Khosravi, M., Sohrabi, M.R., Dastmalchi, S., Gharbani, P.J.J.O.C.P. 2019. Response surface methodology (RSM) modeling to improve removal of Cr

(VI) ions from tannery wastewater using sulfated carboxymethyl cellulose nanofilter. 208, 736–742.

Haji Alhaji, M., Sanaullah, K., Fong Lim, S., Ragai Henry Rigit, A., Hamza, A., Khan, A. 2017. Modeling and optimization of photocatalytic treatment of pre-treated palm oil mill effluent (POME) in a UV/$TiO_2$ system using response surface methodology (RSM). Cogent Engineering, 4, 1382980.

Kalavathy, S., Giridhar, M. 2016. A Study on the use of Alum for turbidity removal in Synthetic water. In 3rd National Conference on Water, Environment and Society (NCWES), 263–266.

Kang, L.-S., Cleasby, J.L. 1995. Temperature effects on flocculation kinetics using Fe (III) coagulant. Journal of Environmental Engineering, 121, 893–901.

Karchiyappan, T., Karri, R.R. 2021. Process optimization and modeling of hydraulic fracturing process wastewater treatment using aerobic mixed microbial reactor via response surface methodology. In Soft Computing Techniques in Solid Waste and Wastewater Management, 351–363.

Miron, A.-R., Modrogan, C., Orbulet, O.D., Costache, C., Popescu, I. 2010. Treatment of acid blue 25 containing wastewaters by electrocoagulation. UPB Scientific Bulletin, Series B, 72, 93–100.

Nayeri, D., Mousavi, S.A. 2020. Treatment of highly turbid water in disaster conditions using coagulation-flocculation process: Modeling and optimization. Water Quality Research Journal, 55, 358–369.

Pal, S., Mukherjee, S., Ghosh, S. 2014. Optimum phenol sorption in peat by the response surface method. Environmental Geotechnics, 1, 142–151.

Perec, A. 2021. Multiple response optimization of abrasive water jet cutting process using response surface methodology (RSM). Procedia Computer Science, 192, 931–940.

Rachidi, L., Kaichouh, G., Khachani, M., Zarrouk, A., Karbane, M.E., Chakchak, H., Warad, I., Hourch, A.E.L., Kacemi, K.E., Guessous, A. 2021. Optimization and modeling of the electro-Fenton process for treatment of sertraline hydrochloride: Mineralization efficiency, energy cost and biodegradability enhancement. Chemical Data Collections, 35, 100764.

Rohani, S., Went, J., Duvenhage, D.F., Gerards, R., Wittwer, C., Fluri, T. 2021. Optimization of water management plans for CSP plants through simulation of water consumption and cost of treatment based on operational data. Solar Energy, 223, 278–292.

Salehi, Z., Vahabzadeh, F., Sohrabi, M., Fatemi, S., Znad, H.T. 2010. Statistical medium optimization and biodegradative capacity of ralstonia eutropha toward p-nitrophenol. Biodegradation, 21, 645–657.

Senthil Kumar, P., Centhil, V., Kameshwari, R., Palaniyappan, M., Kalaivani, V.D., Pavithra, K.G. 2016. Experimental study on parameter estimation and mechanism for the removal of turbidity from groundwater and synthetic water using Moringa oleifera seed powder. Desalination Water Treatment, 57, 5488–5497.

Shi, B., Wei, Q., Wang, D., Zhu, Z., Tang, H. 2007. Coagulation of humic acid: The performance of preformed and non-preformed Al species. Colloids Surfaces A: Physicochemical Engineering Aspects, 296, 141-148.

Thirugnanasambandham, K., Sivakumar, V., Prakash Maran, J. 2015. Performance evaluation and optimization of electrocoagulation process to treat grey wastewater. Desalination Water Treatment, 55, 1703–1711.

Trinh, T.K., Kang, L.S. 2010. Application of response surface method as an experimental design to optimize coagulation tests. Environmental Engineering Research, 15, 63–70.

Usefi, S., Asadi-Ghalhari, M. 2019. Modeling and optimization of the coagulation–flocculation process in turbidity removal from aqueous solutions using rice starch. Pollution, 5, 623–636.

Xiao, F., Huang, J.-C.H., Zhang, B.-J., Cui, C.-W. 2009. Effects of low temperature on coagulation kinetics and floc surface morphology using alum. Desalination, 237, 201–213.

Zainal-Abideen, M., Aris, A., Yusof, F., Abdul-Majid, Z., Selamat, A., Omar, S. 2012. Optimizing the coagulation process in a drinking water treatment plant–comparison between traditional and statistical experimental design jar tests. Water Science Technology, 65, 496–503.